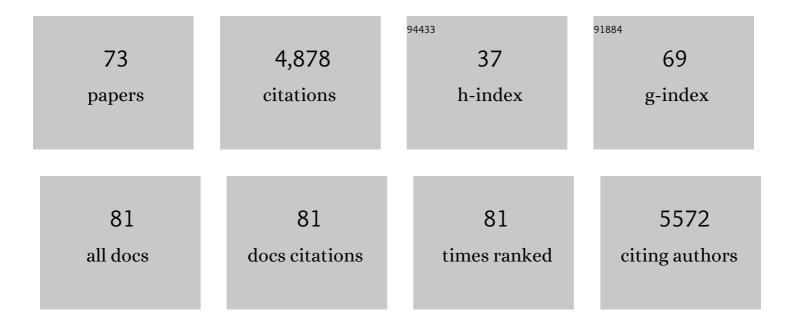
Aleix Comas-Vives

List of Publications by Year in descending order

Source: https://exaly.com/author-pdf/5746857/publications.pdf Version: 2024-02-01



ALEIN COMAS-VINES

#	Article	IF	CITATIONS
1	Activity Trends in the Propane Dehydrogenation Reaction Catalyzed by MIII Sites on an Amorphous SiO2 Model: A Theoretical Perspective. Topics in Catalysis, 2022, 65, 242-251.	2.8	1
2	Understanding the Olefin Polymerization Initiation Mechanism by Cr(III)/SiO ₂ Using the Activation Strain Model. Journal of Physical Chemistry C, 2022, 126, 296-308.	3.1	6
3	A combined experimental and computational study to decipher complexity in the asymmetric hydrogenation of imines with Ru catalysts bearing atropisomerizable ligands. Catalysis Science and Technology, 2021, 11, 2497-2511.	4.1	6
4	Strain in Silica-Supported Ga(III) Sites: Neither Too Much nor Too Little for Propane Dehydrogenation Catalytic Activity. Inorganic Chemistry, 2021, 60, 6865-6874.	4.0	20
5	Dynamics and Site Isolation: Keys to High Propane Dehydrogenation Performance of Silica-Supported PtGa Nanoparticles. Jacs Au, 2021, 1, 1445-1458.	7.9	32
6	Shape and Surface Morphology of Copper Nanoparticles under CO2 Hydrogenation Conditions from First Principles. Journal of Physical Chemistry C, 2021, 125, 396-409.	3.1	15
7	Engineering the Cu/Mo2CTx (MXene) interface to drive CO2 hydrogenation to methanol. Nature Catalysis, 2021, 4, 860-871.	34.4	138
8	Oxygen Electronic Character at the Interface Tunes Catalytic Selectivity. CheM, 2020, 6, 2865-2868.	11.7	2
9	Dynamic Pd ^{II} /Cu ^I Multimetallic Assemblies as Molecular Models to Study Metal–Metal Cooperation in Sonogashira Coupling. Chemistry - A European Journal, 2020, 26, 12168-12179.	3.3	23
10	Design of an Accurate Machine Learning Algorithm to Predict the Binding Energies of Several Adsorbates on Multiple Sites of Metal Surfaces. ChemCatChem, 2020, 12, 4611-4617.	3.7	24
11	Atomically Dispersed Iridium on Indium Tin Oxide Efficiently Catalyzes Water Oxidation. ACS Central Science, 2020, 6, 1189-1198.	11.3	47
12	Bulk and Nanocrystalline Cesium Lead-Halide Perovskites as Seen by Halide Magnetic Resonance. ACS Central Science, 2020, 6, 1138-1149.	11.3	43
13	Hydrogenolysis of Polysilanes Catalyzed by Lowâ€Valent Nickel Complexes. Angewandte Chemie, 2020, 132, 15733-15739.	2.0	1
14	Hydrogenolysis of Polysilanes Catalyzed by Lowâ€Valent Nickel Complexes. Angewandte Chemie - International Edition, 2020, 59, 15603-15609.	13.8	11
15	Exploiting two-dimensional morphology of molybdenum oxycarbide to enable efficient catalytic dry reforming of methane. Nature Communications, 2020, 11, 4920.	12.8	78
16	CO ₂ Hydrogenation on Cu/Al ₂ O ₃ : Role of the Metal/Support Interface in Driving Activity and Selectivity of a Bifunctional Catalyst. Angewandte Chemie, 2019, 131, 14127-14134.	2.0	21
17	CO ₂ Hydrogenation on Cu/Al ₂ O ₃ : Role of the Metal/Support Interface in Driving Activity and Selectivity of a Bifunctional Catalyst. Angewandte Chemie - International Edition, 2019, 58, 13989-13996.	13.8	112
18	Viewpoint: Atomic-Scale Design Protocols toward Energy, Electronic, Catalysis, and Sensing Applications. Inorganic Chemistry, 2019, 58, 14939-14980.	4.0	23

ALEIX COMAS-VIVES

#	Article	IF	CITATIONS
19	Facile Fischer–Tropsch Chain Growth from CH ₂ Monomers Enabled by the Dynamic CO Adlayer. ACS Catalysis, 2019, 9, 6571-6582.	11.2	20
20	What Can We Learn from First Principles Multi-Scale Models in Catalysis? The Role of the Ni/Alâ,,Oâ,ƒ Interface in Water-Gas Shift and Dry Reforming as a Case Study. Chimia, 2019, 73, 239.	0.6	3
21	CO methanation on ruthenium flat and stepped surfaces: Key role of H-transfers and entropy revealed by ab initio molecular dynamics. Journal of Catalysis, 2019, 371, 270-275.	6.2	15
22	Proton-Detected Multidimensional Solid-State NMR Enables Precise Characterization of Vanadium Surface Species at Natural Abundance. Journal of Physical Chemistry Letters, 2019, 10, 7898-7904.	4.6	12
23	Taming Radical Intermediates for the Construction of Enantioenriched Trifluoromethylated Quaternary Carbon Centers. Angewandte Chemie - International Edition, 2019, 58, 1447-1452.	13.8	50
24	Taming Radical Intermediates for the Construction of Enantioenriched Trifluoromethylated Quaternary Carbon Centers. Angewandte Chemie, 2019, 131, 1461-1466.	2.0	20
25	Decisive Role of Perimeter Sites in Silica-Supported Ag Nanoparticles in Selective Hydrogenation of CO ₂ to Methyl Formate in the Presence of Methanol. Journal of the American Chemical Society, 2018, 140, 13884-13891.	13.7	37
26	Electronic Structure–Reactivity Relationship on Ruthenium Step-Edge Sites from Carbonyl 13C Chemical Shift Analysis. Journal of Physical Chemistry Letters, 2018, 9, 3348-3353.	4.6	9
27	Adlayer Dynamics Drives CO Activation in Ru-Catalyzed Fischer–Tropsch Synthesis. ACS Catalysis, 2018, 8, 6983-6992.	11.2	29
28	CO ₂ â€toâ€Methanol Hydrogenation on Zirconiaâ€Supported Copper Nanoparticles: Reaction Intermediates and the Role of the Metal–Support Interface. Angewandte Chemie - International Edition, 2017, 56, 2318-2323.	13.8	435
29	Cooperativity and Dynamics Increase the Performance of NiFe Dry Reforming Catalysts. Journal of the American Chemical Society, 2017, 139, 1937-1949.	13.7	322
30	Understanding surface site structures and properties by first principles calculations: an experimental point of view!. Chemical Communications, 2017, 53, 4296-4303.	4.1	16
31	CO ₂ â€ŧoâ€Methanol Hydrogenation on Zirconiaâ€Supported Copper Nanoparticles: Reaction Intermediates and the Role of the Metal–Support Interface. Angewandte Chemie, 2017, 129, 2358-2363.	2.0	51
32	Strain effect and dual initiation pathway in CrIII/SiO2 polymerization catalysts from amorphous periodic models. Journal of Catalysis, 2017, 346, 50-56.	6.2	46
33	Contrasting the Role of Ni/Al ₂ O ₃ Interfaces in Water–Gas Shift and Dry Reforming of Methane. Journal of the American Chemical Society, 2017, 139, 17128-17139.	13.7	172
34	Role of Coordination Number, Geometry, and Local Disorder on ²⁷ Al NMR Chemical Shifts and Quadrupolar Coupling Constants: Case Study with Aluminosilicates. Journal of Physical Chemistry C, 2017, 121, 19946-19957.	3.1	28
35	Molecular Structure and Confining Environment of Sn Sites in Single-Site Chabazite Zeolites. Chemistry of Materials, 2017, 29, 8824-8837.	6.7	44
36	Olefin polymerization on Cr(III)/SiO2: Mechanistic insights from the differences in reactivity between ethene and propene. Journal of Catalysis, 2017, 354, 223-230.	6.2	24

#	Article	IF	CITATIONS
37	Role of Water, CO ₂ , and Noninnocent Ligands in the CO ₂ Hydrogenation to Formate by an Ir(III) PNP Pincer Catalyst Evaluated by Static-DFT and ab Initio Molecular Dynamics under Reaction Conditions. Organometallics, 2017, 36, 4908-4919.	2.3	18
38	Local Structures and Heterogeneity of Silica-Supported M(III) Sites Evidenced by EPR, IR, NMR, and Luminescence Spectroscopies. Journal of the American Chemical Society, 2017, 139, 8855-8867.	13.7	58
39	X–H Bond Activation on Cr(III),O Sites (X = R, H): Key Steps in Dehydrogenation and Hydrogenation Processes. Organometallics, 2017, 36, 234-244.	2.3	51
40	Increased Back-Bonding Explains Step-Edge Reactivity and Particle Size Effect for CO Activation on Ru Nanoparticles. Journal of the American Chemical Society, 2016, 138, 16655-16668.	13.7	67
41	Role of Tricoordinate Al Sites in CH ₃ ReO ₃ /Al ₂ O ₃ Olefin Metathesis Catalysts. Journal of the American Chemical Society, 2016, 138, 6774-6785.	13.7	42
42	Correlating Synthetic Methods, Morphology, Atomic-Level Structure, and Catalytic Activity of Sn-β Catalysts. ACS Catalysis, 2016, 6, 4047-4063.	11.2	106
43	Surface Sites in Cu-Nanoparticles: Chemical Reactivity or Microscopy?. Journal of Physical Chemistry Letters, 2016, 7, 3259-3263.	4.6	30
44	CO ₂ Activation on Ni/γ–Al ₂ O ₃ Catalysts by First-Principles Calculations: From Ideal Surfaces to Supported Nanoparticles. ACS Catalysis, 2016, 6, 4501-4505.	11.2	92
45	Intrinsic reactivity of Ni, Pd and Pt surfaces in dry reforming and competitive reactions: Insights from first principles calculations and microkinetic modeling simulations. Journal of Catalysis, 2016, 343, 196-207.	6.2	156
46	Predictive morphology, stoichiometry and structure of surface species in supported Ru nanoparticles under H ₂ and CO atmospheres from combined experimental and DFT studies. Physical Chemistry Chemical Physics, 2016, 18, 1969-1979.	2.8	36
47	Amorphous SiO ₂ surface models: energetics of the dehydroxylation process, strain, ab initio atomistic thermodynamics and IR spectroscopic signatures. Physical Chemistry Chemical Physics, 2016, 18, 7475-7482.	2.8	128
48	Surface Organometallic and Coordination Chemistry toward Single-Site Heterogeneous Catalysts: Strategies, Methods, Structures, and Activities. Chemical Reviews, 2016, 116, 323-421.	47.7	650
49	The Effect of the Electronic Nature of Spectator Ligands in the C–H Bond Activation of Ethylene by Cr(III) Silicates: An ab initio Study. Chimia, 2015, 69, 225.	0.6	4
50	Carbon–Carbon Bond Formation by Activation of CH ₃ F on Alumina. Journal of Physical Chemistry C, 2015, 119, 7156-7163.	3.1	28
51	Reply to Peters et al.: Proton transfers are plausible initiation and termination steps on Cr(III) sites in ethylene polymerization. Proceedings of the National Academy of Sciences of the United States of America, 2015, 112, E4162-3.	7.1	16
52	Heterolytic Activation of C–H Bonds on Cr ^{III} –O Surface Sites Is a Key Step in Catalytic Polymerization of Ethylene and Dehydrogenation of Propane. Inorganic Chemistry, 2015, 54, 5065-5078.	4.0	103
53	Cooperativity between Al Sites Promotes Hydrogen Transfer and Carbon–Carbon Bond Formation upon Dimethyl Ether Activation on Alumina. ACS Central Science, 2015, 1, 313-319.	11.3	92
54	NMR Signatures of the Active Sites in Snâ€Î²â€Zeolite. Angewandte Chemie, 2014, 126, 10343-10347.	2.0	46

#	Article	IF	CITATIONS
55	Silica-surface reorganization during organotin grafting evidenced by 119Sn DNP SENS: a tandem reaction of gem-silanols and strained siloxane bridges. Physical Chemistry Chemical Physics, 2014, 16, 17822-17827.	2.8	40
56	NMR Signatures of the Active Sites in Snâ€Î²â€Zeolite. Angewandte Chemie - International Edition, 2014, 53, 10179-10183.	13.8	157
57	Proton transfers are key elementary steps in ethylene polymerization on isolated chromium(III) silicates. Proceedings of the National Academy of Sciences of the United States of America, 2014, 111, 11624-11629.	7.1	118
58	Ab initio study of the electrochemical H ₂ SO ₄ /Pt(111) interface. Physical Chemistry Chemical Physics, 2013, 15, 992-997.	2.8	21
59	CO oxidation on stepped-Pt(111) under electrochemical conditions: insights from theory and experiment. Physical Chemistry Chemical Physics, 2013, 15, 18671.	2.8	16
60	Unraveling the Pathway of Gold(I)-Catalyzed Olefin Hydrogenation: An Ionic Mechanism. Journal of the American Chemical Society, 2013, 135, 1295-1305.	13.7	53
61	Multiscale Modeling of Au-Island Ripening on Au(100). Advances in Physical Chemistry, 2011, 2011, 1-11.	2.0	9
62	How Important Is Backbonding in Metal Complexes Containing Nâ€Heterocyclic Carbenes? Structural and NBO Analysis. European Journal of Inorganic Chemistry, 2011, 2011, 5025-5035.	2.0	80
63	A Computational Study of the Olefin Epoxidation Mechanism Catalyzed by Cyclopentadienyloxidomolybdenum(VI) Complexes. Chemistry - A European Journal, 2010, 16, 2147-2158.	3.3	84
64	The Wacker Process: Inner―or Outerâ€Sphere Nucleophilic Addition? New Insights from Ab Initio Molecular Dynamics. Chemistry - A European Journal, 2010, 16, 8738-8747.	3.3	55
65	Inner- and Outer-Sphere Hydrogenation Mechanisms: A Computational Perspective. Advances in Inorganic Chemistry, 2010, 62, 231-260.	1.0	34
66	Mechanistic evaluation of metal-catalyzed hydrogen-transfer processes: The Shvo catalyst as an example of computational unravelling. Computational and Theoretical Chemistry, 2009, 903, 123-132.	1.5	41
67	Mechanistic analogies and differences between gold- and palladium-supported Schiff base complexes as hydrogenation catalysts: A combined kinetic and DFT study. Journal of Catalysis, 2008, 254, 226-237.	6.2	29
68	Theoretical Analysis of the Hydrogen-Transfer Reaction to Câ•N, Câ•C, and C≡C Bonds Catalyzed by Shvo's Ruthenium Complex. Organometallics, 2008, 27, 4854-4863.	2.3	44
69	Hydrogen Transfer to Ketones Catalyzed by Shvo's Ruthenium Hydride Complex:  A Mechanistic Insight. Organometallics, 2007, 26, 4135-4144.	2.3	130
70	Nature of Cp*MoO2+in Water and Intramolecular Proton-Transfer Mechanism by Stopped-Flow Kinetics and Density Functional Theory Calculations. Inorganic Chemistry, 2007, 46, 4103-4113.	4.0	39
71	Single-Site Homogeneous and Heterogeneized Gold(III) Hydrogenation Catalysts:Â Mechanistic Implications. Journal of the American Chemical Society, 2006, 128, 4756-4765.	13.7	161
72	Self-Assembly of Mercaptaneâ^'Metallacarborane Complexes by an Unconventional Cooperative Effect:Â A Câ^'H···Sâ^'H··AHâ^'B Hydrogen/Dihydrogen Bond Interaction. Journal of the American Chemical Society, 2005, 127, 15976-15982.	13.7	105

#	Article	IF	CITATIONS
73	Kinetic Monte Carlo simulations of the Dry reforming of Methane catalyzed by the Ru (0001) Surface based on Density Functional Theory calculations. Catalysis Science and Technology, 0, , .	4.1	2